Analytical chemistry of synthetic routes to psychoactive tryptamines Part II.† Characterisation of the Speeter and Anthony synthetic route to *N*,*N*-dialkylated tryptamines using GC-EI-ITMS, ESI-TQ-MS-MS and NMR‡

Simon D. Brandt,[a] Sally Freeman,[b] Ian A. Fleet,[c] Peter McGagh[a] and John F. Alder*[a]

Received 23rd August 2004, Accepted 3rd December 2004
First published as an Advance Article on the web 13th January 2005
DOI: 10.1039/b413014f

The degree of alkylation of the side chain nitrogen in tryptamines is one important factor that affects psychoactivity. The method of Speeter and Anthony is considered to be one of the most important synthetic preparative methods. The final step in this reaction is based on the reduction of a (substituted) indole-3-yl-glyoxalylamide to the desired tryptamine with metal hydride. Twelve symmetrically and 13 asymmetrically *N*,*N*-disubstituted glyoxalylamides and their corresponding tryptamine derivatives have been synthesised and characterised by gas chromatography EI-ion trap mass spectrometry, electrospray-triple quadrupole-tandem mass spectrometry and NMR spectroscopy. Mass spectral and NMR similarities and differences between the investigated compounds are discussed. A solvent dependency is observed that has to be taken into consideration for the unambiguous assignment of ^{1}H- and ^{13}C-NMR chemical shifts. The ^{1}H-NMR study demonstrated that one can evaluate the rotamer populations of the asymmetrical glyoxalylamides. In a forensic or clinical scenario where single or multiple reaction monitoring approaches are contemplated, the appropriate ion transitions of choice may then focus on the two main fragmentations, namely β-cleavage ($[M+H]^+ \rightarrow CH_2N^+R^2R^3$) and/or α-cleavage ($[M+H]^+ \rightarrow$ [3-vinylindole]$^+$), respectively. The synthesis, NMR and MS analytical data presented provide the forensic analyst and clinical biochemist with a detailed and self-consistent body of information and mechanisms for the spectral identification of the more likely psychoactive tryptamines that may be met.

Introduction

Several tryptamine derivatives are known to induce altered states of consciousness and the term ''hallucinogens'' is commonly used for this type of compound in an attempt to describe their powerful impact on human perception, mood and cognition. These simple indolealkylamine alkaloids, which are abundantly found in many plants and fungi, have been used since ancient times for recreational and religious purposes.[1,2] In recent years there has been an increased interest in human clinical research on the effect of several dimethylated tryptamine derivatives, such as dimethyltryptamine (DMT)[3–6] and psilocybin [4-(H_2O_3PO)DMT].[7–9] The current understanding of basic neuropharmacological actions and the implications on possible future neuroscientific research has recently been reviewed by Nichols.[10] Psychoactivity is greatly affected by substitution on the indole ring, the side-chain carbons and by alkylation of the side-chain nitrogen. Most of the psychoactive *N*,*N*-disubstituted derivatives known may show oral activity, presumably due to their lack of sufficient substrate-specificity to the metabolising enzyme monoamine oxidase. Homologation of the *N*,*N*-dialkyl substituents however, appears to diminish potency.[11–14]

Liquid chromatography-atmospheric pressure mass spectrometry (LC-API-MS(-MS)) has found a wide range of applications in recent years which showed its complementary value when compared with more traditional techniques, such as GC-EI-MS.[15–17] Indeed, the use of an electrospray ionisation source (ESI) enabled the analysis of thermally labile tryptamines such as psilocybin, which decomposes easily *via* dephosphorylation to psilocin (4-HO-DMT) when introduced into a hot injector of a GC.[16] The direct detection of psilocybin has been shown by LC-ESI-MS-MS[18] and LC-atmospheric pressure chemical ionisation-MS (LC-APCI-MS).[19] The first direct detection of the urinary metabolite of psilocin, psilocin-*O*-glucuronide, by LC-ESI-MS-MS has also recently been described.[20]

The synthetic route of Speeter and Anthony[21,22] involves acylation of a (substituted) indole with oxalyl chloride followed by reaction with an amine to give an indole-3-yl-glyoxalylamide. This amide is then reduced with lithium aluminium hydride to tryptamines (Scheme 1). The combination of in-source fragmentation with ESI-triple quadrupole-tandem MS (ESI-TQ-MS-MS) has recently been used in this laboratory for the identification of several impurities during the synthesis of 5-methoxy-*N*,*N*-diisopropyltryptamine (5-MeO-DIPT), a psychoactive tryptamine derivative.[23]

† For Part I see ref. 23.
‡ Electronic supplementary information (ESI) available: Supplementary data, tables and figures. See http://www.rsc.org/suppdata/an/b4/b413014f/
*fred.alder@umist.ac.uk

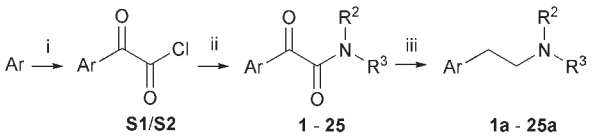

Scheme 1 Synthesis of *N*,*N*-disubstituted tryptamine derivatives *via* the synthetic route of Speeter and Anthony. i: Oxalyl chloride; ii: (secondary) amine; iii: $LiAlH_4$; $R^2 = R^3 =$ alkyl or H; Ar = 5-methoxyindole or indole. For structures of glyoxalylamides **1–25** and tryptamines **1a–25a**: see Table 1.

In the present study the characterisation of this synthetic route has been extended to 12 symmetrically and 13 asymmetrically *N*,*N*-disubstituted glyoxalylamides and their corresponding tryptamines. Mass spectral characterisation involved the comparison of GC-EI-ion trap-MS (GC-EI-ITMS), ESI-time of flight-MS (ESI-TOF-MS) and ESI-TQ-MS-MS of both amide intermediates and tryptamines. A detailed NMR study is also presented which provides information on the rotamer populations for the 13 asymmetrically *N*,*N*-disubstituted glyoxalylamides.

Experimental

Materials

Anhydrous ether (99.8%), 5-methoxyindole (99%), indole (98%), anhydrous THF (99.9%), $LiAlH_4$ (95%), $CDCl_3$, and all appropriate amines were from Aldrich UK. *N*-Ethyl-*N*-propylamine and *N*-ethyl-*N*-isobutylamine were from Alfa Aesar (Karlsruhe, Germany). Other solvents and reagents used were of analytical or HPLC grade. P_2O_5 (98%), silica gel (40–63 μm), and d_6-DMSO (Uvasol grade) were from VWR UK.

Instrumentation

Nuclear magnetic resonance NMR spectra were recorded using a Bruker DPX 400 at 399.9 MHz (^{1}H-NMR) or 100.6 MHz (^{13}C-NMR), unless stated otherwise (Bruker DPX 300) at 300 K. The solvent used was d_6-DMSO and ^{1}H chemical shifts were calibrated on residual solvent at 2.51/39.6 ppm, unless stated otherwise. Melting points have been determined using a SMP3 melting point apparatus (Stuart Scientific, UK) and are uncorrected.

Table 1 Structures, GC-MS retention times and exact masses for synthesised starting materials **S1** and **S2**, *N*,*N*-disubstituted glyoxalylamides **1–25** and their corresponding tryptamines **1a–25a**

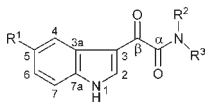

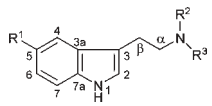

					[M+H]$^+$				[M+H]$^+$	
Compound	R^1	R^2	R^3	^{t}R/min[a]	Theory	Observed[b]	Compound	^{t}R/min[a]	Theory	Observed[b]
S1	MeO	—	—	—[c]	220.0610	220.0617[d]				
S2	H	—	—	—[c]	190.0504	190.0509[d]				
1	MeO	n-Bu	n-Bu	33.00	331.2022	331.2028	**1a**	13.51	303.2436	303.2437
2	H	n-Bu	n-Bu	22.05	301.1916	301.1922	**2a**	10.63	273.2331	273.2332
3	MeO	Et	Et	19.37	275.1396	275.1399	**3a**	9.76	247.1810	247.1808
4	H	Et	Et	13.86	245.1290	245.1297	**4a**	8.27	217.1705	217.1702
5	MeO	i-Bu	i-Bu	26.37	331.2022	331.2014	**5a**	12.14	303.2436	303.2437
6	H	i-Bu	i-Bu	18.24	301.1916	301.1908	**6a**	9.82	273.2331	273.2325
7	MeO	i-Pr	i-Pr	21.98	303.1709	303.1710	**7a**	10.98	275.2123	275.2112
8	H	i-Pr	i-Pr	15.35	273.1603	273.1600	**8a**	9.06	245.2018	245.2011
9[e]	MeO	Me	Me	16.63	269.0902	269.0907	**9a**	8.77	219.1497	219.1489
10	H	Me	Me	12.22	217.0977	217.0976	**10a**	7.62	189.1392	189.1393
11	MeO	n-Pr	n-Pr	24.34	303.1709	303.1716	**11a**	11.12	275.2123	275.2115
12	H	n-Pr	n-Pr	16.91	273.1603	273.1590	**12a**	9.20	245.2018	245.2009
13	MeO	Et	i-Pr	20.96	289.1552	289.1548	**13a**	10.32	261.1967	261.1957
14	H	Et	i-Pr	14.84	259.1447	259.1441	**14a**	8.63	231.1861	231.1861
15	MeO	Et	n-Pr	21.72	289.1552	289.1560	**15a**	10.42	261.1967	261.1968
16	H	Et	n-Pr	15.31	259.1447	259.1448	**16a**	8.70	231.1861	231.1856
17[e]	MeO	H	i-Pr	16.07	283.1059	283.1061	**17a**	9.32	233.1654	233.1648
18	MeO	Me	Et	18.11	261.1239	261.1234	**18a**	9.28	233.1654	233.1659
19	H	Me	Et	13.08	231.1134	231.1131	**19a**	7.96	203.1548	203.1545
20	MeO	Me	i-Bu	22.15	289.1552	289.1561	**20a**	10.18	261.1967	261.1957
21	H	Me	i-Bu	15.52	259.1447	259.1443	**21a**	8.55	231.1861	231.1851
22	MeO	Me	i-Pr	19.95	275.1396	275.1387	**22a**	9.90	247.1810	247.1803
23	H	Me	i-Pr	14.20	245.1290	245.1287	**23a**	8.36	217.1705	217.1697
24	MeO	Me	n-Pr	20.63	275.1396	275.1389	**24a**	9.89	247.1810	247.1800
25	H	Me	n-Pr	14.59	245.1290	245.1301	**25a**	8.35	217.1705	217.1702

[a] GC-MS retention times in minutes using a 30 m, 5% phenyl capillary column (see Procedures for details). [b] Exact masses were determined by ESI-TOF-MS with an experimental error <5 ppm. [c] Thermal degradation in the injector. [d] Observed as hydrolysed acid derivative in the electrospray interface (see text). [e] Observed as [M+Na]$^+$.

A Varian (USA) 1200L triple quadrupole MS equipped with an ESI interface was used and controlled by the MS Workstation version 6.30. A LC system provided the solvent system using two ProStar 210 solvent delivery modules. The solvent system consisted of (A) 0.1% v/v aqueous formic acid and (B) acetonitrile and was run isocratically at 50% A and B. Flow injection analysis was carried out with 20 μg ml^{-1} solutions (for compounds **1–25**) and 10 μg ml^{-1} solutions (compounds **1a–25a**), respectively, dissolved in the mobile phase. MS parameters: Drying and nebulizing gas was nitrogen at 20 psi and 350 °C, and 41 psi, respectively. The collision gas was argon and collision induced dissociation (CID) took place at 1.2 mTorr at 42 °C. The needle was held at 5000 V, shield at 600 V and the capillary voltage was 35 V. In-source CID experiments were performed with an increased capillary voltage as described in the text. For tandem MS experiments quadrupole 1 (Q_1) was set for the appropriate protonated molecular ion $[M+H]^+$ and the collision energy of collision cell q_2 (rf only) was set to 0 eV. Fragmentation was induced by applying an appropriate potential described in the text. The scan time was 1 s in positive mode (centroid) and the detector multiplier voltage was set to 1275 V.

A Micromass LCT orthogonal acceleration time-of-flight TOF mass spectrometer (Micromass, UK) equipped with an electrospray ionisation source was operated in positive mode. Samples were introduced using a flow injection method, *via* a Waters 2790 separation module autosampler. The instrument was tuned and calibrated in the mass range 100 to 1000 Da using 10 nl ml^{-1} PEG 300 + 10 nl ml^{-1} PEG 600 in 50 : 50 acetonitrile/water containing 2 mM ammonium acetate and 0.1% v/v formic acid. Exact mass measurements were carried out after instrument calibration using either caffeine (3 μg ml^{-1}) or leucine enkephaline (4 μg ml^{-1}) as lock mass standards. All electrospray data were obtained at sample concentrations of 5 μg ml^{-1}.

Electron ionisation mass spectra were obtained on a Varian Saturn 2200 ion trap MS equipped with a Varian CP-3800 gas chromatograph (Varian, USA) and a Combi Pal autosampler (CTC Analytics, Switzerland). Data handling was completed with Saturn GC/MS Workstation, Version 5.52 software. A 5% phenyl, 30 m × 0.25 mm CP-Sil 8 CB Low Bleed/MS column with a film thickness of 0.25 μm was used. The column temperature was programmed as follows: 40 °C and hold 1 min, then heat at 50 °C min^{-1} to 260 °C and hold for 14.6 min. Total run time was 20 min for the analysis of tryptamine derivatives and 50 min for the analysis of glyoxalylamide derivatives. A CP-1177 injector (280 °C) was used in the split mode with a 50 : 1 split. The carrier gas was helium at a flow rate of 1 ml min^{-1} (EFC constant flow mode). The mass spectrometer was run in the EI auto mode at 70 eV over a mass range of 20–400 amu with a scan time of 0.5 s. The transfer line, manifold and ion trap temperatures were set to 300 °C, 95 °C and 200 °C, respectively.

Procedures

Synthesis (Scheme 1). The identities of the synthesised compounds (Table 1) were confirmed by exact mass measurements (experimental error below 5 ppm) and NMR spectroscopy. NMR spectra were obtained by ^{1}H-NMR, proton decoupled ^{13}C, distortionless enhancement polarisation transfer (DEPT-135) and ^{1}H–^{13}C COSY (heteronuclear multiple quantum coherence, HMQC) experiments. Some of the analytical data referred to can be found in the electronic supplementary information (ESI): Figs. S1, S2 and Tables S1–S4.‡ The indole ^{1}H-NMR and ^{13}C-NMR chemical shifts are given in Tables 6–9, S3 and S4,‡ respectively. All other chemical shifts that were measured in d_6-DMSO, melting points (for **1–25**) and yields are also provided in the ESI.‡ Characterisation of tryptamine derivatives **1a–25a** is based on the free base. The rotamer ratios are given in Table 2.

Step 1: General procedure for the synthesis of glyoxalyl chloride derivatives **S1** and **S2**

The appropriate indole (5.44 mmol; 5-methoxyindole: 800 mg; indole: 637 mg) was dissolved in 150 ml anhydrous ether and stirred on ice for 30 min. Oxalyl chloride (2.07 g, 16.3 mmol) was added dropwise, stirred for 30 min on ice and kept at −20 °C for 4 h. The orange and yellow α-oxo acid chlorides **S1/S2** were filtered and washed three times with 50 ml cold anhydrous ether and dried *in vacuo* for 3 h at room

Table 2 Estimation of the rotameric ratio found in asymmetrically *N*,*N*-disubstituted glyoxalylamides **13–25** based on ^{1}H-NMR integrals at 300 °K in d_6-DMSO and $CDCl_3$[a]

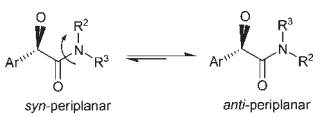

Solvent	Compound	**13**	**14**	**15**	**16**	**17**	**18**	**19**	**20**	**21**	**22**	**23**	**24**	**25**
	Small (R^2)	Et	Et	Et	Et	H	Me	Me	Me	Me	Me	Me	Me	Me
	Large (R^3)	i-Pr	i-Pr	n-Pr	n-Pr	i-Pr	Et	Et	i-Bu	i-Bu	i-Pr	i-Pr	n-Pr	n-Pr
	Anti (%)	70	68	55	54	100	58	56	52	51	67	66	53	52
d_6-DMSO	*Syn* (%)	30	32	45	46	0	42	44	48	49	33	34	47	48
	Anti (%)	69	68	53	53	100	58	59	52	51	ns[b]	67	55	55
$CDCl_3$	*Syn* (%)	31	32	47	47	0	42	41	48	49	ns[b]	33	45	45

[a] Glyoxalylamides **13–25** are asymmetrically substituted on the amide side chain nitrogen which results in the existence of different rotamer populations. Steric effects (R^2 = small-size substituent; R^3 = large-size substituent) lead to the predominance of one major rotamer, presumably represented by an *anti*-periplanar orientation towards the amide group. [b] ns: not sufficiently soluble. Formation of unequal rotamer populations is observed in ^{1}H-NMR spectra as unequivalent, *i.e* partial, integrals. The estimation (±2%) is based on the peak height of the side chain protons (see Procedures section). No significant solvent dependency is observed.

temperature to give a yield of 1.19 g (5.00 mmol, 92%) for **S1** and 1.02 g (4.90 mmol, 90%) for **S2**. Both compounds were used for the next step without further purification (for analytical data refer to ESI‡).

Step 2: General procedure for the synthesis of *N*,*N*-disubstituted glyoxalylamide derivatives **1–25**

The appropriate amine (15.65 mmol) was added dropwise to an ice-cold solution of 5-methoxyindole-3-yl-glyoxalyl chloride **S1** (1.24 g, 5.22 mmol) or indole-3-yl-glyoxalyl chloride **S2** (1.08 g, 5.22 mmol) dissolved in 100 ml anhydrous THF. The mixture was stirred on ice for 4 h. The solvent was evaporated under reduced pressure to give a crude solid that was purified by flash chromatography (DCM-MeOH, 9 : 1). The solvent was evaporated under reduced pressure and all products **1–25** were recrystallised from ethyl acetate and dried overnight under vacuum over P_2O_5, unless stated otherwise (for analytical data refer to ESI‡).

Step 3: General procedure for the synthesis of *N*,*N*-disubstituted tryptamine derivatives **1a–25a**

A solution of the appropriate glyoxalylamide **1–25** (1.5 mmol), in 40 ml anhydrous THF, was added dropwise to a stirred, ice-cold slurry of lithium aluminium hydride (570 mg, 15 mmol) in 100 ml anhydrous THF under nitrogen. This reaction mixture was heated at reflux for 15 h and then cooled on ice. The excess hydride was destroyed by the dropwise addition of 5 ml water, followed by 5 ml 20% NaOH and 5 ml of water. The precipitated inorganic salts were filtered and washed 3 times with 30 ml THF. The filtrate was evaporated under reduced pressure and the resulting oily residue was dissolved in 75 ml DCM and washed three times with water and once with saturated aqueous NaCl. The organic phase was dried over anhydrous $MgSO_4$ and evaporated under reduced pressure. The resulting oils were dried overnight *in vacuo* over P_2O_5 to yield the desired, mostly solid, tryptamine derivatives **1a–25a** (for analytical data refer to ESI‡).

Results and discussion

Glyoxalylamides **1–25** and the corresponding tryptamines **1a–25a** were synthesised by the route of Speeter and Anthony (Scheme 1). Chemical structures and GC-MS retention times are provided in Table 1.

Mass spectrometry

EI-ITMS of glyoxalylamides

The EI-induced fragmentation of 5-methoxy-*N*,*N*-disubstituted glyoxalylamides (5MGs) produces a characteristic key pattern that bears some resemblance to the fragmentation of indole-3-carboxylic acid derivatives.[24] Scheme 2A provides an overview of the proposed fragmentation pathway. The base peak in 5MGs is always represented by an ion at *m*/*z* 174 and may correspond to an indole-CO structure (**b2**). This species undergoes cleavage of CO and CH_3 as represented by fragments *m*/*z* 146 (**c2**) and *m*/*z* 159 (**d2**), respectively. Scheme 2A also shows that a species at *m*/*z* 131 may have been generated *via* different pathways and therefore

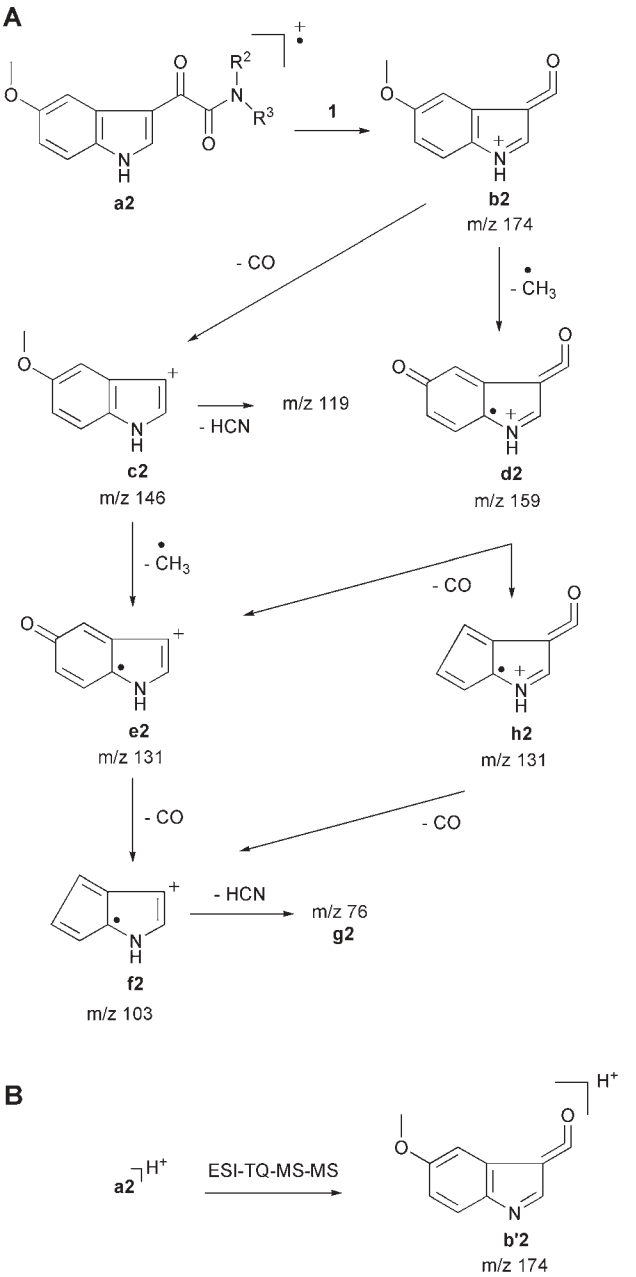

Scheme 2 A: Proposed key fragmentation pattern of 5-methoxy-*N*,*N*-disubstituted glyoxalylamides under EI-ITMS conditions (R^2 = R^3 = alkyl). Pathway **1** leads to a 5-methoxyindole-CO+ fragment **b2** that represents the base peak in all cases. The *m*/*z* 131 fragment may be formed by several different fragmentations. B: A similar key fragment **b′2** is observed after collision-induced dissociation of **a2** using ESI-triple quadrupole tandem mass spectrometry.[23]

represented by different structures (**e2**, **h2**). For example, the ion at *m*/*z* 146 (**c2**, 5-methoxyindole-*H*) may lose a methyl radical that generates fragment **e2** (*m*/*z* 131). This resonance-stabilised dihydro-5-indolone ion, in turn, loses CO and may form a ring-contracted fragment at *m*/*z* 103 (**f2**). The expulsion of HCN would then account for the presence of the species at *m*/*z* 76 (**g2**). In summary, the key fragmentation pattern of all investigated 5MGs gives rise to the following series of *m*/*z* 174, *m*/*z* 159, *m*/*z* 146, *m*/*z* 131, *m*/*z* 103 and *m*/*z* 76.

N,*N*-Disubstituted glyoxalylamides that are unsubstituted on the benzene ring (UGs) produce an equivalent fragmentation pattern. The base peak at *m*/*z* 144 may be subsequently represented by an analogous oxo-methylene structure that is shown in Scheme 2A for 5MGs. Since UGs do not posses a 5-methoxy substituent a less complex spectrum is observed. The base peak fragment *m*/*z* 144 may lose CO which gives rise to an [indole-H]$^+$ at *m*/*z* 116 that, in turn, is thought to expel HCN and forms a species at *m*/*z* 89. The UGs therefore generate a key pattern of *m*/*z* 144, *m*/*z* 116 and *m*/*z* 89.

Table 3 shows the EI-induced mass spectra of all synthesised glyoxalylamides **1–25** and enables the comparison between isomeric compounds. The relative abundance of the odd electron molecular ions is found to vary between 1–10% (not shown) whereas the relative intensities of the key fragments in both groups (5MGs and UGs) appear to be relatively stable without being influenced by structural modifications. Some isomeric glyoxalylamides produce indistinguishable mass spectra such as the *N*,*N*-dibutyl- and *N*,*N*-diisobutyl derivatives **1/5** and **2/6**, respectively. The EI-MS of the remaining derivatives appear to exhibit minor differences and may therefore allow their differentiation. For example the *N*,*N*-dipropyl derivative **11** can be differentiated from its *N*,*N*-diisopropyl isomer **7** by the presence of a fragment at *m*/*z* 217. The corresponding compounds that are unsubstituted on the benzene ring (**12** and **8**) produce an equivalent ion at *m*/*z* 187, the identity of this fragment however, is unknown. Interestingly, the *N*-ethyl-*N*-propyl derivatives (**15**, **16**) do also show this fragment in their mass spectra, in contrast to the *N*-methyl-*N*-propyl (**24**, **25**) and *N*-methyl-*N*-isopropyl compounds (**22**, **23**), respectively.

During an investigation of the EI-MS of several psychoactive drug classes, Bellman and coworkers found a fragment at *m*/*z* 173 for derivative **4**.[25] It has been attributed to an α-type cleavage with following hydrogen transfer from the amine group to the oxygen.[25] As shown in Table 3 the same fragment is also observed in other derivatives that contain at least one ethyl substituent such as **14** and **19**. The corresponding mass-shifted 5-methoxy- fragment is found, albeit weak, in the EI-MS of **3**, **13** and **18** at *m*/*z* 203. As shown in Table 1 unambiguous assignments of isomeric glyoxalylamides may also be performed by the comparison of GC-MS retention times.

ESI-TQ-MS-MS of glyoxalylamides

The full scan spectrum of a directly infused glyoxalylamide derivative exhibits a base peak at [M+H]$^+$ unless the CID gas was introduced into the collison cell. The most intense peak then is found to be [M+Na]$^+$. The full scan of an ESI-TOF-MS reveals a base peak at [M+acetonitrile+Na]$^+$ instead. [2M+Na]$^+$ ($\sim$50% relative intensity) and [3M+Na]$^+$ ions ($\sim$5% relative intensity) are also generally found in ESI-TOF-MS. The complexation with sodium ions is presumably favoured by the presence of the two carbonyl groups and a slightly higher concentration of 20 μg ml^{-1} is used for direct infusion into the

Table 3 EI-ITMS spectra of *N*,*N*-disubstituted glyoxalylamides **1–25**[a]

Relative intensity (%) of generated key fragment ions								
		Key pattern of 5-methoxy-*N*,*N*-disubstituted glyoxalylamides (5MGs)						Other fragments *m*/*z* (%)
Compound	M^b	Base peak	*m*/*z* 159	*m*/*z* 146	*m*/*z* 131	*m*/*z* 103	*m*/*z* 76	
1	330	174	10	8	9	4	3	231 (9), 128 (15), 57 (10)
5	330	174	9	8	9	4	4	231 (5), 128 (21), 57 (11)
7	302	174	11	9	10	5	6	100 (26), 86 (12)
11	302	174	11	9	11	5	4	217 (9), 100 (12)
13	288	174	13	10	12	5	6	203 (3), 86 (22), 72 (9)
15	288	174	11	10	11	5	6	217 (6), 203 (4), 86 (11), 72 (5)
20	288	174	10	9	10	5	5	86 (10)
3	274	174	13	10	10	6	6	203 (12), 72 (16)
22	274	174	14	11	12	5	6	72 (18), 58 (7)
24	274	174	14	10	12	5	6	76 (6)
17	260	174	13	10	11	6	6	119 (4), 76 (5)
18	260	174	16	11	13	8	9	203 (3), 119 (5), 76 (8), 58 (18)
9	246	174	16	12	13	6	7	119 (5), 72 (13)
		Key pattern of *N*,*N*-disubstituted glyoxalylamides (UGs)						Other fragments *m*/*z* (%)
Compound	M^b	Base peak	*m*/*z* 116		*m*/*z* 89			
2	300	144	22		18			201 (3), 128 (24), 57 (14)
6	300	144	20		13			201 (4), 128 (28), 57 (14)
8	272	144	26		23			100 (39), 86 (18), 63 (8), 58 (5)
12	272	144	24		22			187 (11), 100 (19), 63 (6)
14	258	144	23		21			173 (4), 86 (31), 72 (11), 63 (8)
16	258	144	24		19			187 (7), 173 (4), 86 (17), 63 (7)
21	258	144	22		19			86 (15), 63 (6), 57 (6)
4	244	144	25		21			173 (17), 100 (7), 72 (21), 63 (8)
23	244	144	27		23			72 (27), 63 (8), 58 (9)
25	244	144	22		18			72 (11), 71 (9), 63 (7)
19	230	144	27		23			173 (8), 63 (10), 58 (27),
10	216	144	31		23			72 (16), 63 (10)

[a] The key fragment ions of compounds **1–25** are listed in the order of their molecular masses to allow a direct mass spectral comparison between isomers. [b] Odd electron molecular ion.

electrospray interface in order to compensate for a slightly reduced signal intensity in the ESI-TQ instrument.

The fragmentation pattern of the investigated 5MGs are generally identical to that of compound **7** which has been reported previously.[23] Briefly, the key fragmentation process is characterised by the dissociation of the protonated molecular ion $[M+H]^+$ also into a [5-methoxyindole-CO+H]$^+$ species at *m*/*z* 174 (**b′2**) or, in case of the unsubstituted glyoxalylamide counterpart, into an [indole-CO+H]$^+$ fragment at *m*/*z* 144. This dissociation is also observed to a certain extent even without the application of any collision energy. The *m*/*z* 174 ion starts to fragment at collision energies around 15–20 eV. A loss of CO may give rise to an ion at *m*/*z* 146 and loss of CH_3 may produce a species at *m*/*z* 159. The *m*/*z* 159 ion may subsequently lose CO (*m*/*z* 131) whereas fragment *m*/*z* 146 may also expel CH_3 (*m*/*z* 131) and HCN (*m*/*z* 119) (see ref. 23 for a proposed fragmentation pathway). A corresponding dissociation reaction is observed for the tandem MS of UGs. Here, the key fragmentation process is characterised by the dissociation of *m*/*z* 144 to *m*/*z* 116 (loss of CO) and subsequent cleavage of HCN which leads to an ion at *m*/*z* 89.

Table S1‡ summarises the CID mass spectra that have been obtained at a collision energy of 10 eV. As mentioned above the base peak (*m*/*z* 174 or *m*/*z* 144, respectively) corresponds to the appropriate [indole-CO+H]$^+$ fragment. Two additional ions are observed. As indicated in Table S1‡ the fragments that show a slightly higher relative abundance may be represented by a $[HNR^2R^3+H]^+$ species which may suggest an α-cleavage of the CON-bond. The second additional fragment may be rationalised by a $[CONR^2R^3]^+$ species. Increasing the collision energy is not found to contribute to a more significant or distinct fragmentation pattern. Rather, the dissociation of the base peak fragment is instigated which, as expected, appears to be similar for all glyoxalylamides as discussed above (Scheme 2A). Although both of these two species appear at relatively low collision energies, *i.e.* 10 eV, their appearance could not be reproduced by in-source fragmentation in order to investigate possible differential dissociations by tandem MS. It appears therefore, that under these conditions isomeric compounds cannot be distinguished when using ESI-TQ-MS-MS. The only exception, however is found for *N*,*N*-diisopropyl derivatives **7** and **6** that are characterised by the cleavage of propene from the side chain, thus leading to the fragments at *m*/*z* 261 and *m*/*z* 231 respectively. This neutral loss is not seen in *N*,*N*-dipropyl derivatives **11** and **12** respectively.

Both acid chlorides **S1** and **S2** although relatively stable, cannot be detected directly by this technique due to their conversion into the corresponding α-oxo-acetic acid derivative in the electrospray interface. This has been described previously for **S1** and its 5-benzyloxy-derivative.[23] Here, the presence of the unsubstituted acid derivative has been confirmed by exact mass measurements using ESI-TOF-MS and correspondingly, the nominal mass of $[M+H]^+$ is found to be 190 Da. Similarly, its dissociation takes place *via* [indole-CO+H]$^+$ at *m*/*z* 144 as described above. Also, both **S1** and **S2** display thermal instability and are not found to produce suitable GC-MS data under the conditions used.

EI-ITMS of tryptamines

The EI-induced fragmentation of 5-methoxy-*N*,*N*-disubstituted tryptamines (5MTs) produces a characteristic key pattern that is in agreement with previous investigations conducted on a limited number of these derivatives. This pattern has been interpreted based on the detection of metastable ions and deuteration experiments as summarised in Scheme 3.[26–28] Tertiary amines produce a base peak that results from a β-cleavage where the charge resides on the nitrogen of this fragment $[H_2C{=}NR^2R^3]^+$ (**d3**). This β-cleavage can also lead to a fragment at *m*/*z* 160 where the charge is attached to the indolic fragment (**e3**). An α-cleavage produces an ion at *m*/*z* 174 that in turn can expel a methylene radical in order to give the *m*/*z* 160 fragment. It has been reported that this uncommon loss was supported by metastable ion transitions.[26] Holmstedt and Lindgren have considered an alternative tricyclic structure for *m*/*z* 174 (**c3**).[29] The *m*/*z* 160 ion **e3** which can be considered as a 5-methoxyindole-methylene ion, has been suggested to undergo a rearrangement that yields an expanded, resonance-stabilised quinolinium ion **e′3**. This is analogous to the formation of tropylium ions in the context of the fragmentation behaviour of several alkyl benzenes.[30] The following fragmentations are consistent with the behaviour of methoxy group-bearing indoles,[24] *i.e.* loss of methyl (*m*/*z* 145, **g3**), CO (*m*/*z* 117, **h3**) and HCN (*m*/*z* 90, **i3**). The species at *m*/*z* 130 (**f3**) has been attributed to the loss of formaldehyde based on metastable data.[26] Hattox and Murphy however, did not find this corresponding transition. Interestingly, it has been reported that loss of formaldehyde was only favoured when the methoxy group was present either at positions 4 or 7 or when an *ortho* substituent next to the methoxy group was present.[31] The presence of fragment *m*/*z* 130 (**f3**), however, may be difficult to rationalise without the loss of formaldehyde from its precursor at *m*/*z* 160 (**e3**). In summary the characteristic fragmentation pattern of 5MTs shows, apart from the base peaks, the following series of key fragments: *m*/*z* 174, *m*/*z* 160, *m*/*z* 145, *m*/*z* 130, *m*/*z* 117 and *m*/*z* 90. This pattern is clearly distinguishable from the unsubstituted tryptamine derivatives (see below). This is particularly helpful in cases where the molecular ion is absent or very weak, a phenomenon that is known for the mass spectra of disubstituted derivatives.[26]

The mass spectrum of secondary 5MTs exhibit an additional feature which is attributed to monosubstitution of the side chain nitrogen. Compound **17a** may serve as an example: the base peak of this compound is not the usual $[CH_2NR^2R^3]^+$ after β-cleavage but a fragment at *m*/*z* 161. Bosin and coworkers attributed its formation to a McLafferty rearrangement (**k3**) when discussing the mass spectrum of the primary 5-methoxytryptamine.[32] Such a mechanism also appears reasonable in a secondary tryptamine, such as **17a**, since a specific transfer of a γ-hydrogen in a six-membered transition state would be ensured (**a′3**).[33] A skeletal rearrangement, similar to that observed for *m*/*z* 160 (**e′3**) mentioned above, leads to a 2,3-dehydroquinolinium structure (**j3**) followed by loss of a hydrogen that produces the aromatic quinolinium fragment **e′3** at *m*/*z* 160.[26,28] *N*-Methyltryptamine derivatives, for example, have been found to exhibit a similar mass spectral

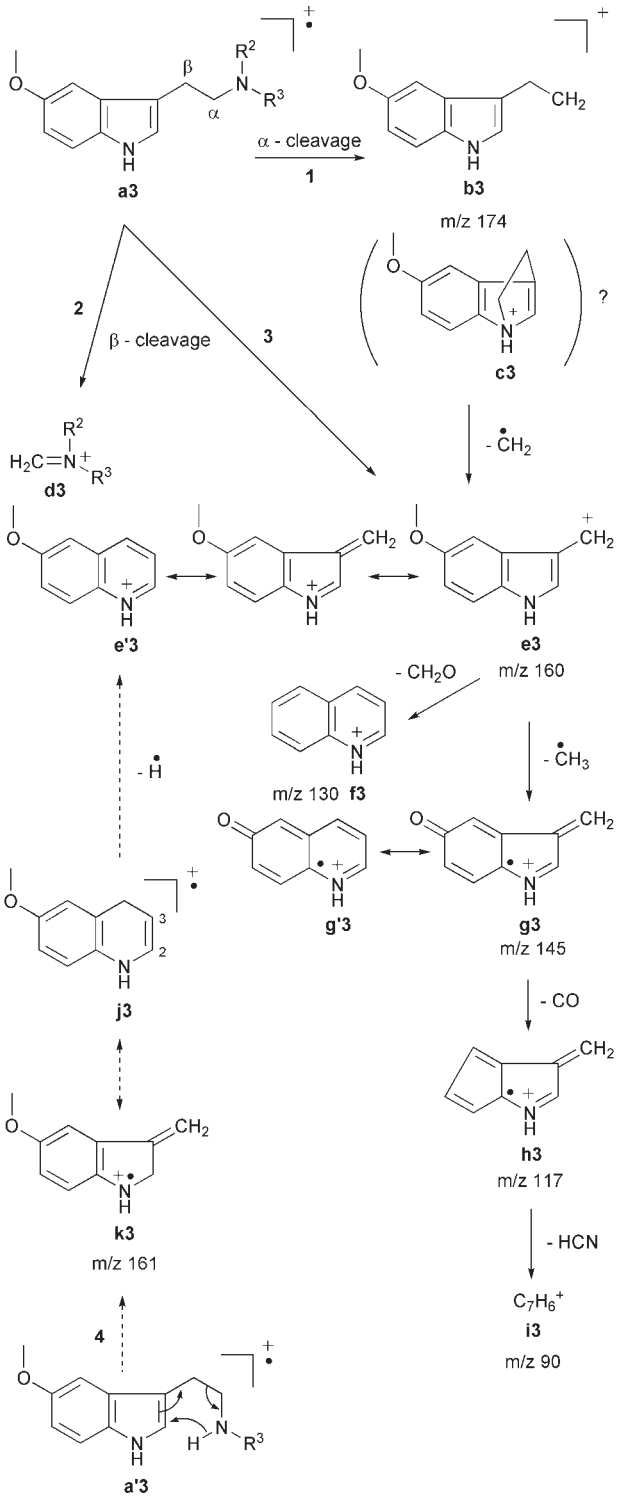

Scheme 3 Key fragmentation pattern of 5-methoxy-*N*,*N*-disubstituted derivatives under EI-MS conditions (R^2 = R^3 = alkyl). The mass spectrum is dominated by the base peak of fragment **d3** that results from pathway **2** *via* β-cleavage. Part of the characteristic fragmentation pattern is the occurrence of ions **b3**, **e3**, **g3**, **h3**, **i3** with a relative intensity of ~10% and **f3** (~5%), formed *via* pathway **1** (α-cleavage) or **3**. An additional fragmentation is observed for secondary derivatives of **a3** (**a′3**, R^2 = H, R^3 = alkyl). Fragment **j3** is formed *via* a McLafferty-type rearrangement which in turn is converted to **e′3** (see text for details).

feature regarding the non-aromatic/aromatic quinolinium relationship.[34]

The EI-induced mass spectral pattern of unsubstituted tryptamine derivatives (UTs) appears to be more straightforward due to the lack of the methoxy group but shows similar principles. A similar α-cleavage is observed that yields an ion at *m*/*z* 144. The β-cleavage produces the same base peak [M-$CH_2NR^2R^3$]$^+$ and a corresponding indole-methylene ion at *m*/*z* 130 which is also thought to rearrange to the aromatic quinolinium ion. A major difference between the pattern discussed above and here is the loss of HCN already from the quinolinium ion that results in a fragment at *m*/*z* 103 and it has been suggested that this ion ($C_8H_7^+$) may exist as a styryl cation.[30] Loss of acetylene gives rise to a phenyl cation ($C_6H_5^+$) at *m*/*z* 77. The characteristic key pattern for UTs is therefore observed in the following series: *m*/*z* 144 *m*/*z* 130, *m*/*z* 103 and *m*/*z* 77.

Table 4 shows the EI-MS spectra of the synthesised tryptamines **1a–25a** in order of their molecular masses. This allows a direct comparison of the fragmentation behaviour of isomeric tryptamines. In 5MTs the relative intensities of the characteristic key fragments (Scheme 3) display slight fluctuations, ranging approximately between 1–15%. The mass spectrum of the secondary 5MT derivative **17a**, however, shows higher relative intensities for these ions. A similar trend for the relative abundances is observed for UTs. Here, the quinolinium ion at *m*/*z* 130 generally displays a slightly higher abundance compared to the ions at *m*/*z* 144, *m*/*z* 103 and *m*/*z* 77.

It is also apparent from Table 4 that isomeric tryptamines can be differentiated. The iminium ion [CH_2=$N^+R^2R^3$ ≅ $C_nH_{2n+2}N^+$, also often termed "immonium"] (**d3**), which represents the base peak in all tertiary tryptamines (R^2 = R^3 = alkyl) fragments under these conventional EI conditions. These secondary decompositions depend on the substituents on the nitrogen and are characterised for example, by hydrogen rearrangements and olefin eliminations (C_nH_{2n}).[35,36] To the best of our knowledge however, the monitoring of iminium ions under mass spectral conditions, either by EI-MS or ESI-TQ-MS-MS, has not been described for the differentiation of tryptamine derivatives. The observed fragmentations are in agreement with previous investigations on olefin eliminations from some isolated iminium ions based on ^{2}H-labelling and metastable data derived from aliphatic amines.[36,37] For example, the asymmetric *N*-methyl-*N*-propyltryptamine derivatives **24a/25a** (MPTs) can be differentiated from isomeric *N*-methyl-*N*-isopropyltryptamines **22a/23a** (MIPTs) and from *N*,*N*-diethyltryptamines **3a/4a** (DETs) by the fragmentation of their iminium ions at *m*/*z* 86 (Table 4). The fragmentation of the CH_2=$N^+(CH_3)C_3H_7$ ion (*m*/*z* 86, derived from MPTs) is characterised by the loss of propene and ethene. The iminium ion that corresponds to MIPTs in contrast, eliminates only propene and therefore no fragment at *m*/*z* 58 is observed. Interestingly it has been suggested that the expulsions of propene in both cases may differ mechanistically.[37] In the second case, a stable (*i.e.* no isomerisation) isopropyl cation may be formed which has been suggested to take part in an ion-neutral complex (INC). A specific β-H transfer to the nitrogen, presumably *via* a

Table 4 EI-ITMS spectra of *N*,*N*-disubstituted tryptamines **1a–25a**[a]

Relative intensity (%) of generated key fragment ions													
	Structurally relevant fragment ions *m/z* (%)												
	5-Methoxy-*N*,*N*-disubstituted tryptamines[b]							Characteristic key pattern					
Compound	M+1[c]	Base peak	*m/z* 58	*m/z* 72	*m/z* 86	*m/z* 100	Others *m/z* (%)	*m/z* 174	*m/z* 160	*m/z* 145	*m/z* 130	*m/z* 117	*m/z* 90
1a	303	142	63	0	1	85	44 (14)	6	16	10	5	10	3
5a	303	142	3	0	18	26	44 (12), 57 (16)	9	12	6	5	6	2
7a	275	114	1	39	1	1	—	3	10	8	4	10	4
11a	275	114	11	7	51	0	44 (16)	5	11	8	4	9	3
13a	261	100	60	0	1	100	—	2	8	7	4	10	4
15a	261	100	17	53	1	100	—	4	9	8	4	10	3
20a	261	100	30	0	1	100	57 (20), 44 (56)	10	10	9	5	10	3
3a	247	86	17	0	100	0	—	2	5	5	3	8	3
22a	247	86	0	1	100	0	44 (76)	2	7	7	4	9	4
24a	247	86	59	0	100	0	44 (31)	4	8	8	5	11	5
18a	233	72	0	100	0	1	44 (34)	2	5	6	3	9	4
17a	233	161	1	66	0	1	—	7	38	22	9	29	11
9a	219	58	100	0	0	0	—	1	5	5	3	8	5

	Structurally relevant fragment ions *m/z* (%)										
	N,*N*-Disubstituted tryptamines[b]							Characteristic key pattern			
Compound	M+1[c]	Base peak	*m/z* 58	*m/z* 72	*m/z* 86	*m/z* 100	Others *m/z* (%)	*m/z* 144	*m/z* 130	*m/z* 103	*m/z* 77
	273										
2a	273	142	80	0	0	87	44 (17)	9	27	6	8
6a	245	142	3	0	16	25	44 (14), 57 (16)	13	16	3	5
8a	245	114	1	43	1	1	—	5	16	6	8
12a	231	114	12	7	49	1	44 (20)	6	16	5	7
14a	231	100	62	1	1	100	—	4	15	6	8
16a	231	100	17	59	0	100	—	6	14	6	7
21a	217	100	34	0	0	100	44 (58), 57 (17)	14	15	6	9
4a	217	86	15	0	100	1	—	2	11	5	5
23a	217	86	0	1	100	1	44 (85)	5	12	7	11
25a	203	86	65	0	100	1	44 (30)	6	14	6	11
19a	189	72	0	100	0	1	44 (34)	2	8	4	9
10a		58	100	1	1	0	—	1	7	5	6

[a] Compounds **1a–25a** and their key fragment ions are listed in the order of their molecular masses to allow a direct mass spectral comparison between isomers. [b] These structurally relevant fragment ions may be formed by the fragmentation of the iminium ion (base peak) and allows differentiation between isomeric derivatives. [c] Molecular ion observed as M+1 under these conditions with very low intensity.

proton-bridged complex, may take place which results in the expulsion of propene and the secondary iminium ion $CH_2{=}N^+HCH_3$ (*m/z* 44). The loss of propene from the iminium ion that derives from MPTs has been suggested to display distinct selectivities in hydrogen transfer due to α-H, β-H and γ-H transfers with preceding unidirectional isomerisation of the *N*-n-propyl group to a *N*-isopropyl group.[37,38] These retro-ene reactions of gaseous iminium ions however, have also been suggested to proceed in a concerted, rather than in a stepwise manner.[39] The loss of ethene from $CH_2{=}N^+(C_2H_5)_2$ (DETs) only produces $C_3H_8N^+$ (*m/z* 58, $CH_2N^+H(C_2H_5)$) in moderate intensity and is therefore distinguishable from MPTs since it lacks the $C_2H_6N^+$ fragment at *m/z* 44.

This is of particular interest where similar GC-MS retention times are observed as shown in Table 1, for example for MIPTs (**22a**, **23a**) and MPTs (**24a**, **25a**) that are found to coelute under these experimental conditions. Apart from these compounds it can also be seen in Table 1 that all investigated compounds show sufficiently different retention times (Fig. S1‡). All UTs and 5MTs were mixed and subjected to GC-MS. The resulting chromatograms are shown in Fig. S1A and S1B, respectively.‡ These results show acceptable separation of both tryptamine groups.

The methyleneiminium ions of diisopropyltryptamines (DIPTs) **7a/8a** produce a distinguishable pattern when compared with dipropyltryptamines (DPTs) **11a/12a** (Table 4). In both cases the base peak is observed at *m/z* 114 which, in the case of DIPTs, appears to fragment only into an ion at *m/z* 72 which is in agreement with the findings of Veith and Gross.[36] In the case of the dipropyl substituted ion a loss of ethene may be responsible for the formation of the secondary methyleneiminium fragment $CH_2{=}N^+HPr$ ($C_4H_{10}N^+$) at *m/z* 86. This process is thought to involve a specific γ-H transfer *via* a six-membered transition state where an open-chain carbonium ion undergoes σ-bond cleavage.[40] Additional fragments are found at *m/z* 58 and *m/z* 44. It appears conceivable that this particular secondary *m/z* 86 ion undergoes further tertiary fragmentation in analogy to what has been discussed above for MPTs. A relative abundance of 7% for ion *m/z* 72 in this spectrum may account for the loss of propene (''onium reaction'') from the *N*,*N*-dipropyl substituted iminium ion (Table 4).[36,40]

In general terms, the elimination of alkenes from $C_nH_{2n+2}N^+$ iminium ions presumably proceeds *via* two pathways: Elimination of C_nH_{2n} (loss of the entire alkyl chain, R = C_nH_{2n+1}) or expulsion of an alkene with one carbon less than the alkyl group ($C_{n-1}H_{2n-2}$).[40,41] The fragmentation of the primary methyleneiminium ion (base peak, $CH_2N^+R^2R^3$ = $C_nH_{2n+2}N^+$) may produce a secondary and possibly a tertiary ion. This iminium series thus appears at *m/z* 44, *m/z* 58, *m/z* 72, *m/z* 86 and *m/z* 100 *etc* [16 + 14*n*]. An ion at *m/z* 44 may therefore be represented by $CH_2N^+HCH_3$ ($C_2H_6N^+$), and an ion at *m/z* 58 either by $CH_2N^+HC_2H_5$ or $CH_2N^+(CH_3)_2$ ($C_3H_8N^+$) *etc*.

It is relatively common to obtain M+1 ions when using ITMS (Table 4 for tryptamines) due to ion–molecule interactions. Interestingly, glyoxalylamides are found to display the odd electron molecular ion only as shown in Table 3.

ESI-TQ-MS-MS of tryptamines

Using both, ESI-TOF-MS and ESI-TQ-MS, the investigated tryptamine derivatives produce solely the protonated molecular ion $[M+H]^+$ without any adduct formation. The collision induced dissociation of all 5MTs gives rise to a pattern that has been found during a previous investigation on the characterisation of 5-MeO-DIPT **7a**.[23] Considering the additional confirmatory results in this study, the major mass spectral characteristics are based on the dissociation of the protonated molecular ion $[M+H]^+$ into two main fragments when moderate collision energies are applied. Table S2‡ shows that at collision energies around 12 ± 2 eV maximum intensity of iminium ion fragments are observed ($CH_2{=}N^+R^2R^3$, see EI-MS discussion above). The second main fragment is found at *m/z* 174 and is thought to represent [5-methoxy-3-vinylindole]$^+$ as supported by exact mass measurements (see ref. 23 for a proposed fragmentation pathway). It can also be seen in Table S2‡ that maximum intensity requires slightly higher collision energies around 16 ± 4 eV for this species. A further increase of the collision energy leads to the dissociation of *m/z* 174 into fragments at *m/z* 159 (loss of CH_3) and *m/z* 146 (loss of OCH_3). The *m/z* 159 ion may subsequently lose CO (*m/z* 131) and CHO (*m/z* 130).

Unsubstituted *N*,*N*-disubstituted tryptamines (UTs) also display the two key dissociations described above and as shown in Tables S2‡ and 5. Higher collision energies above 15–20 eV leads to further dissociation of the [3-vinylindole]$^+$ ion at *m/z* 144 which mainly results in the appearance of *m/z* 117 and *m/z* 127. The loss of HCN may be responsible for the presence of *m/z* 117 and a dihydroindene-like structure ($C_9H_9^+$) has been proposed by McClean and coworkers when discussing the ESI-IT-MS-MS-MS of tryptamine.[42] The presence of *m/z* 127 ($C_{10}H_7^+$) however, may only be rationalised by the loss of NH_3 from the vinylindole fragment. The production of the *m/z* 144 by in-source fragmentation (100 V capillary voltage) and subsequent tandem MS (collison energy 30 eV) yields a slightly more complex spectrum, mainly characterised by additional abundant ions at *m/z* 116, *m/z* 115, *m/z* 91, *m/z* 90, *m/z* 89 and *m/z* 77. The last four fragments may represent typical aromatic hydrocarbons that are normally encountered in EI-MS,[26] such as the tropylium ion at *m/z* 91 ($C_7H_7^+$).[43]

As discussed in the EI-MS section, isomeric tryptamines are found to exhibit differential EI-induced mass spectra (Table 4), due to secondary and tertiary fragmentations of the base peak-producing iminium ions. To investigate further this possibility under ESI-TQ-MS-MS conditions the appropriate unsubstituted tryptamine derivative was subjected to in-source fragmentation by increasing the capillary voltage from 35 V to 85 V. Under these conditions the protonated molecular ion dissociates into the iminium ion ($CH_2{=}N^+R^2R^3$) and the

Table 5 CID mass spectra of iminium ions using in-source fragmentation and ESI-TQ-MS-MS in positive mode[a]

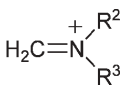

No.	Derived from compound[b]	R^2	R^3	Precursor *m/z* (%)	Product ions *m/z* (%)	
					Alkene elimination	Imine elimination
I	**1a** & **2a**	n-Bu	n-Bu	142 (40)	100 (100), 58 (37), 44 (2)	57 (9)
II	**5a** & **6a**	i-Bu	i-Bu	142 (100)	100 (47), 86 (50)	57 (49)
III	**7a** & **8a**	i-Pr	i-Pr	114 (100)	72 (75), 30 (5)	43 (21)
IV	**11a** & **12a**	n-Pr	n-Pr	114 (100)	86 (67), 72 (27), 58 (7)	43 (17)
V	**13a** & **14a**	Et	i-Pr	100 (75)	58 (100)	43 (22)
VI	**15a** & **16a**	Et	n-Pr	100 (100)	72 (51), 58 (59)	43 (27)
VII	**20** & **21a**	Me	i-Bu	100 (100)	58 (14), 44 (40)	57 (89)
VIII	**3a** & **4a**	Et	Et	86 (100)	58 (31)	43 (63), 29
IX	**22a** & **23a**	Me	i-Pr	86 (100)	44 (83)	—
X	**24a** & **25a**	Me	n-Pr	86 (100)	58 (33), 44 (42)	43 (56)
XI[d]	**18a** & **19a**	Me	Et	72 (100)	44 (42), 30 (8)	—
XII	**17a**	H	i-Pr	72 (59)	—	43 (100)
XIII	**9a** & **10a**	Me	Me	58 [d]	—[d]	—[d]

[a] Iminium ions (see Precursor column) were generated from the corresponding tryptamine using in-source fragmentation. The capillary voltage was increased to 85 V (instead of the usual 35 V). Iminium ions, $CH_2N^+R^2R^3$, were mass-selected in quadrupole 1 (Q_1) and subjected to CID by the application of a collision energy of 15 eV in the second rf-only quadrupole (q_2). Fragments were scanned in quadrupole 3 (Q_3) and thus leading to MS^3. [b] Refers to the tryptamine derivative that generates the iminium ion, *i.e.* 5-methoxy- or unsubstituted on the benzene ring, after α-cleavage. [c] Capillary voltage of 60 V was applied. [d] No satisfactory signal intensity achieved for the iminium precursor by in-source fragmentation.

[3-vinylindole]$^+$ (*m*/*z* 174 for 5MTs or *m*/*z* 144 for UTs, respectively). As mentioned above (Table S2‡) this process is also observed under moderate CID conditions. In this context, the readily produced iminium ion was mass-selected in the first quadrupole and subjected to CID in the collision cell (q_2). For all iminium ions a collision energy of 15 eV has been applied; the product ions were scanned with Q_3. This combination of in-source CID with TQ-MS-MS generates a MS-MS-MS scenario and therefore increases the information content of a mass spectral investigation. The results of this approach are shown in Table 5 where iminium ions with similar masses are grouped together to facilitate the comparison of their product ions. Two main features are observed. Firstly, collision-induced dissociation of the generated iminium ions appears to cause alkene eliminations (C_nH_{2n}) that have also been observed in conventional EI mass spectra (Table 4) as mentioned above. The corresponding product ions may therefore be smaller $C_nH_{2n+2}N^+$ ions. Secondly, however, a major difference between most of the EI-induced mass spectra is observed which may also facilitate the differentiation between isomers. The presence of fragments at *m*/*z* 29 (**VIII**, Table 5), *m*/*z* 43 (**III**–**VI**, **VIII**, **X** and **XII**) and *m*/*z* 57 (**I**, **II** and **VII**) may indicate an imine elimination process which generates a $[C_nH_{2n+1}]^+$ species. In this scenario, $CH_2{=}N^+R^2R^3$ iminium ions would expel a neutral imine $CH_2N{=}R^2$ and leave the corresponding $[R^3]^+$. This is consistent with similar findings on the CID of ten structurally different $C_4H_{10}N^+$ ions (mostly $R^1R^2N^+HR^3$) that were generated from their respective aliphatic amine precursors.[44] Interestingly, CID also produced several alkane losses (methane and ethane). In this study however, alkane losses and the corresponding presence of $C_nH_{2n}N^+$ ions are not observed under these experimental conditions.

NMR spectroscopy

Due to restricted rotation within the amide group the NMR spectra of glyoxalylamides (**1–16** and **18–25**) shows the duplication of peaks for the side chain signals.[45,46] A similar phenomenon has been observed during the synthesis of psilocin analogues and for *N*,*N*-(disubstituted)-5,6-methylene-dioxyindole-3-yl-glyoxalylamides.[47–49] The presence of the β-keto functional group reduces the electron density on the amide group which increases the rotational barrier when compared with simple amides.[50] Two fundamental differences, however, can be observed between the NMR spectra of **1–12**

Table 6 ^{1}H-NMR chemical shifts (in d_6-DMSO at 400 MHz, unless otherwise stated) δ of the indolic protons of the synthesised glyoxalylamides **1–25** and starting materials **S1** and **S2** in ppm

Compound[a]	NH-1, mu[b]	H-2, mu, J[c]	H-4, mu, J	H-5, mu, J	H-6, mu, J	H-7, mu, J
5-Methoxy						
S1[d]	12.28, br s	8.33, d, 3.4	7.67, d, 2.6	—	6.91, dd, 8.9, 2.5	7.44, d, 9.0
1[e]	12.11, br s	7.92, d, 3.4	7.59, d, 1.5	—	6.91, dd, 8.7, 2.4	7.43, d, 8.7
3[e]	12.14, br s	7.96, s	7.59, br s	—	6.91, dd, 8.9, 2.4	7.43, d, 8.7
5[e]	12.10, br s	7.91, s	7.65, d, 2.3	—	6.91, dd, 8.8, 2.4	7.44, d, 8.7
7	12.09, br s	7.91, s	7.59, d, 2.3	—	6.90, dd, 8.7, 2.6	7.45, d, 9.0
9	12.20, br s	8.03, s	7.60, d, 2.0	—	6.91, dd, 9.0, 2.5	7.43, d, 8.5
11	12.22, br s	7.94, s	7.60, d, 1.5	—	6.91, dd, 8.8, 2.5	7.44, d, 9.0
13	12.15, br s	7.97, s; 7.95, s	7.59, br s	—	6.91, dd, 8.5, 2.5	7.44, d, 9.0
15	12.15, br s	7.93, s; 7.95, s	7.59, br s	—	6.71, dd, 9.0, 2.5	7.44, d, 9.0
17	12.11, br s	8.64, s	7.74, d, 2.6	—	6.90, dd, 8.9, 2.5	7.43, d, 9.0
18[e]	12.19, br s	8.03, s; 7.98, s	7.61, d, 1.9	—	6.91, dd, 8.7, 2.3	7.43, d, 8.7 7.44, d, 9.0
20	12.26, br s	7.92, s; 8.01, s	7.62, d, 2.5 7.59, d, 1.5	—	6.91, dd, 9.0, 2.5 6.90, dd, 8.5, 2.5	7.44, d, 8.5 7.42, d, 8.0
22	12.20, br s	8.05, s; 7.97, s	7.61, br s	—	6.91, dd, 9.0, 2.5	7.43, d, 9.0 7.44, d, 8.5
24	12.18, br s	8.03, s; 7.96, s	7.60, d, 2.5 7.62, d, 2.5	—	6.93–6.89, m	7.43, d, 8.5 7.44, d, 9.0
Unsubstituted						
S2[d]	12.45, br s	8.42, d, 3.5	8.17, dd, 6.5, 2.0	7.31–7.25, m	7.31–7.25, m	7.55, dd, 6.5, 2.0
2	12.25, br s	8.01, s	8.10, d, 7.0	7.25, td, 7.0, 1.3	7.28, td, 7.0, 1.5	7.54, dd, 6.8, 1.8
4	12.28, br s	8.06, s	8.10, d, 7.5	7.25, td, 7.0, 1.5	7.29, td, 7.0, 1.0	7.54, d, 7.5
6	12.23, br s	8.00, s	8.13, d, 7.5	7.25, td, 7.0, 1.0	7.28, td, 7.5, 1.5	7.54, d, 7.0
8	12.21, br s	8.00, d, 2.5	8.12, d, 7.0	7.25, td, 7.0, 1.0	7.29, td, 7.3, 1.5	7.56, d, 7.0
10	12.33, br s	8.13–8.11, m	8.13–8.11, m	7.26, td, 7.0, 1.5	7.29, td, 7.0, 1.8	7.54, dd, 6.5, 1.8
12	12.26, br s	8.02, s	8.11, d, 7.0	7.25, td, 6.8, 1.0	7.28, td, 7.3, 1.5	7.54, d, 7.0
14	12.26, br s	8.06, s; 8.03, s	8.10, d, 7.5	7.25 , td, 7.0, 1.5	7.29, td, 7.3, 1.5	7.54, d, 7.0
16	12.24, br s	8.02, s; 8.03, s	8.10, d, 7.0	7.26, t, 6.5	7.29, t, 7.0	7.54, d, 6.5
19	12.30, br s	8.11, s; 8.06, s	8.11–8.06, m	7.30–7.23, m	7.30–7.23, m	7.56–7.52, m
21	12.22, br s	8.09, s; 8.01, s	8.12, dd, 6.5, 2.0 8.10, dd[f]	7.32–7.23, m	7.32–7.23, m	7.55, dd, 7.6, 1.5 7.53, dd, 6.8, 1.5
23	12.27, br s	8.14, s; 8.06, s	8.11, br d, 7.0	7.30–7.24, m	7.30–7.24, m	7.54, dd, 7.0, 2.0
25	12.25, br s	8.11, s; 8.04, s	8.13–8.10, m	7.31–7.23, m	7.31–7.23, m	7.56–7.52, m

[a] The top group of compounds are for the 5-methoxy-*N*,*N*-disubstituted glyoxalylamides, whereas the bottom group of compounds are for the unsubstituted *N*,*N*-disubstituted glyoxalylamides (5-H). Glyoxalylamides **13–25** are asymmetrically substituted on the amide side chain nitrogen which results in the existence of different rotamer populations. The chemical shift of the major rotamer is given first. [b] Multiplicity. [c] Coupling constant in Hz. [d] **S1**: Starting material, 5-methoxyindole-3-yl-glyoxalyl chloride. **S2**: Starting material, indole-3-yl-glyoxalyl chloride. [e] 300 MHz. [f] Peak is overlapping with singlet at 8.09 ppm.

and **13–25** (see ESI‡ and Tables 6 and 7). Glyoxalylamides **1–12** are symmetrically substituted on the nitrogen, *i.e.* $R^2 = R^3$ (Table 1), which restricts the doubling of signals to these alkyl groups, whose integrals are equivalent. In contrast, glyoxalylamides **13–25** are asymmetrically substituted on the nitrogen, *i.e.* $R^2 \neq R^3$ (Table 1), which results in the formation of unequal rotamer populations, due to steric effects (Table 2).

The crystal structure of the 4-benzyloxy-derivative of **8** revealed a twisted, orthogonal orientation of the carbonyl groups with a torsional angle of 81.0(4)°.[50] The amide group and its substituents exhibited a coplanar orientation which in turn was found to have a perpendicular orientation towards the indolyl-CO-α-plane with a torsional angle of 87.5(1)°.[50] In the ^{1}H- and ^{13}C-NMR studies of **13–25** two sets of (unequal) peaks for each rotamer were observed. Most of the indolic protons and carbons, as well as the amide substituents, were observed as two peaks (see ESI‡ and Tables 6 and 7). Table 2 gives the estimated ratios of the rotamers (±2%, *anti*-periplanar and *syn*-periplanar) based on the peak heights of the doubled side chain ^{1}H-NMR signals measured in d_6-DMSO and $CDCl_3$. It is apparent from Table 2 that the greatly impact on the rotamer populations is affected by a *N*-isopropyl substituent as exemplified by compounds **22/23** (67 : 33 and 66 : 34, *anti*-periplanar/*syn*-periplanar) and **13/14** (70 : 30 and 68 : 32, *anti*-periplanar/*syn*-periplanar). Fig. S2‡ gives a representative example of an ^{1}H-NMR spectrum of **22**. This effect is attributed to the bulk of the secondary *N*-isopropyl substituent. Accordingly, *N*-alkyl-*N*-n-propyl- or *N*-alkyl-*N*-isobutyl substitution leads to a less dramatic impact on the rotameric ratio due to the primary N-CH_2-carbon (Table 2).

The aromatic ^{1}H-NMR spectra of the 5-methoxy substituted glyoxalylamides (5MGs) and their 5-methoxy tryptamine counterparts (5MTs) show expected splitting patterns (Tables 6, 9 and S3‡). H-4 appears as a fine doublet due to meta coupling with H-6 ($J_{4,6}$ [5MGs]: 1.5–2.5 Hz; $J_{4,6}$ [5MTs]: 2.0–2.6 Hz). H-6 shows ortho coupling with H-7 and meta coupling with H-4 and appears as a doublet of doublets ([5MGs]: $J_{6,7}$: 8.5–9.0 Hz, $J_{6,4}$: 2.3–2.6 Hz; [5MTs]: $J_{6,7}$: 8.5–8.9 Hz, $J_{6,4}$: 2.3–2.5 Hz). H-7 gives a doublet due to ortho coupling with H-6 ($J_{7,6}$ [5MGs]: 8.5–9.0 Hz; $J_{7,6}$ [5MTs]: 8.5–9.0 Hz). Both compound types however, can be distinguished by the order of their proton chemical shifts: In d_6-DMSO 5MGs display their aromatic resonances in the decreasing order of H-2, H-4, H-7, H-6 compared to H-7, H-2, H-4, H-6 for 5MTs. H-2 appears to be more deshielded in 5MGs due to the presence of the β-carbonyl group which results in a significant downfield shift.

^{13}C-NMR assignments are based on HMQC and HMBC experiments. The carbon signals for C-7 and C-6 of 5MGs in d_6-DMSO (Table 7) appear at similar chemical shifts (0.1–0.3 ppm apart), when compared to the C-7 and C-6 resonances of 5MTs (Δδ *ca.* 1 ppm). In 5MTs the C-6 signal is always more shielded (upfield) than C-7 which facilitates

Table 7 ^{13}C-NMR chemical shifts (in d_6-DMSO at 100 MHz, unless otherwise stated) δ of the indolic carbons of the synthesised glyoxalylamides **1–25** and starting materials **S1** and **S2** in ppm

Compound[a]	C-2	C-3	C-3a	C-4	C-5	C-6	C-7	C-7a
5-Methoxy								
S1[b]	137.9	112.2	126.5	103.0	156.0	113.3	113.5	131.4
1[c]	136.7	113.3	126.2	103.0	156.2	113.5	113.8	132.0
3[c]	136.9	113.2	126.1	103.0	156.2	113.6	113.8	132.0
5[c]	136.7	113.5	126.3	103.3	156.2	113.5	113.7	131.9
7[c]	135.9	112.8	125.8	102.6	155.8	113.3	113.5	131.6
9	137.4	113.1	126.1	102.9	156.2	113.6	113.8	132.1
11	136.8	113.3	126.2	103.0	156.2	113.6	113.8	131.9
13[c]	136.6	113.3, 113.2	126.2, 126.1	103.0, 102.9	156.2	113.7, 113.6	113.8, 113.8	132.0
15	136.8	113.3, 113.2	126.1	102.9	156.2	113.7, 113.6	113.8, 113.8	131.8
17[c]	138.6	112.5	127.5	103.7	156.3	113.1	113.6	131.4
18[c]	137.1, 137.0	113.2, 113.1	126.1	103.0	156.2	113.6, 113.6	113.8	132.0
20	137.1, 136.8	113.4, 113.1	126.2	102.9	156.3, 156.2	114.9, 114.8	113.4	131.9, 131.8
22	137.1, 136.9	113.3, 113.0	126.1	102.9, 102.8	156.2	113.7, 113.6	113.8, 113.7	132.0
24[c]	137.1, 136.9	113.1	126.1	103.0	156.2	113.6, 113.3	113.7, 113.6	132.0
Unsubstituted								
S2[b]	138.1	112.6	125.8	121.4	123.0	124.0	113.0	136.8
2[c]	136.7	113.4	125.3	121.2	122.7	123.7	113.0	137.2
4	137.0	113.3	125.2	121.2	122.8	123.8	113.0	137.2
6[c]	136.8	113.6	125.4	121.3	122.8	123.8	113.0	137.1
8	136.4	113.2	125.3	121.2	122.7	123.8	113.0	137.2
10	137.3	113.3	125.3	122.9	122.9	123.9	113.0	137.3
12[c]	136.8	113.5	125.3	121.2	122.7	123.8	113.0	137.2
14[c]	136.7	113.4, 113.3	125.3, 125.2	121.2	122.8, 122.7	123.8, 123.8	113.0, 113.0	137.2, 137.2
16	136.9	113.4, 113.3	125.2	121.2	122.8	123.9, 123.8	113.0	137.1, 137.1
19	137.2, 137.1	113.4, 113.2	125.2	121.2	122.8	123.9	113.0	137.2
21[c]	137.1, 136.9	113.6, 113.2	125.3	121.3	122.9, 122.8	123.9, 123.8	113.0, 113.0	137.1
23	137.0, 136.9	113.5, 113.2	125.3, 125.2	121.2	122.8	123.8	113.0	137.3
25[c]	137.0	113.5, 113.2	125.3	121.2	122.8	123.8, 123.8	113.0	139.2

[a] The top group of compounds are for the 5-methoxy-*N*,*N*-disubstituted glyoxalylamides, whereas the bottom group of compounds are for the unsubstituted *N*,*N*-disubstituted glyoxalylamides (5-H). Glyoxalylamides **13–25** are asymmetrically substituted on the amide side chain nitrogen which results in the existence of different rotamer populations. [b] **S1**: Starting material, 5-methoxyindole-3-yl-glyoxalyl chloride. **S2**: Starting material, indole-3-yl-glyoxalyl chloride. [c] 75 MHz.

unambiguous assignments if d_6-DMSO is used (Table 8). In $CDCl_3$ a close proximity of C-6 and C-7 is observed (Table S4‡). The assignments may thus be interchanged in these cases. A solvent dependence of ^{13}C-NMR resonance signals of aromatic signals has been reported for several 5-substituted indoles when $CDCl_3$ was compared with d_6-DMSO.[51] Similar observations were made also for C-7 and C-6 of 5MGs which are switched over in $CDCl_3$ (not shown). The impact of d_6-DMSO and $CDCl_3$ on the chemical shifts of the aromatic protons and carbons of tryptamines **1a–25a** is summarised in Tables 8, 9, S3 and S4.‡ In 5MTs the chemical shifts of H-2 and H-4 are observed to be inverted (*i.e.* d_6-DMSO: H-7, H-2, H-4, H-6. $CDCl_3$: H-7, H-4, H-2, H-6).

The aromatic proton spectra of unsubstituted tryptamines (UTs) exhibit a splitting and chemical shift pattern that is similar to indole.[52,53] Table 9 shows that in d_6-DMSO the observed chemical shifts are exhibited in the decreasing order of H-4, H-7, H-2, H-6 and H-5 being the most shielded proton. Both H-4 and H-7 appear as doublets with similar coupling constants ($J_{4,5} = J_{7,6}$ *ca.* 7.0–8.0 Hz). Weak coupling between H-2 and NH ($J_{2,NH}$: 1.5–2.5 Hz) is observed for most of the UTs and 5MTs in d_6-DMSO. In contrast most glyoxalylamides do not show a splitting of the H-2 signal into a doublet. The chemical shifts of UTs are also subject to solvent dependency. In $CDCl_3$ the decreasing order for aromatic protons follows the pattern of H-4, H-7, H-6, H-5 and H-2 as the most shielded proton (Table S3‡). The ^{13}C-NMR assignments of the indole ring have been subject to some controversy, particular those of C-4, C-5 and C-6 that are often found very close to each other.[54,55]

In d_6-DMSO the chemical shifts for C-4 and C-5 in UTs are either the same or very close (Table 8), therefore their exact assignments were impossible. The corresponding assignments in $CDCl_3$ however, are possible as shown in Table S4.‡ A comparison of Tables 8 (d_6-DMSO) and S4‡ ($CDCl_3$) reveals that the chemical shifts of C-2 and C-6 are interchanged which can be identified by the afore-mentioned ^{1}H–^{13}C correlation experiments.

A characteristic difference between all glyoxalylamides and their corresponding tryptamines is found in the chemical shift of the NH proton. The resonance of the former appears to be further downfield when compared to the latter ($\Delta\delta \sim 1.6$ ppm). The electron withdrawing effect of the carbonyl groups in the glyoxalylamides results in a reduced electron density on the indole nitrogen which causes significant deshielding. As indicated in Tables 9 and S3‡ a dramatic solvent impact on the chemical shift of NH for all tryptamines is observed ($\Delta\delta \sim 2.6$ ppm). Lower field chemical shifts are attributed to the dipolar aprotic nature of d_6-DMSO when compared with $CDCl_3$ due to stronger hydrogen bonding.

Another characteristic difference between the aromatic proton spectra of unsubstituted glyoxalylamides (UGs) and UTs is displayed in the order of the chemical shifts where H-2 and H-7 are interchanged. Both H-6 and H-5 in UGs are seen as overlapping triplet of doublets, the only exception being **16** that appears as two triplets. The corresponding signals for the asymmetrical UGs **19**, **21**, **23** and **25** appear as complex multiplets due to the contribution of *syn* and *anti* rotamers as mentioned above. It can be summarised from the NMR data that extrapolations from one solvent to the next must therefore be performed with caution.

The ^{13}C-NMR assigned to the side chain CH_2–CH_2 groups of all tryptamine derivatives are readily identifiable, especially when a DEPT-135 experiment is performed. The α-CH_2 group appears further downfield due to the proximity to the side chain nitrogen that causes deshielding (δ *ca.* 55 ppm). The electron donating properties of the indole ring causes the CH_2-β group to be more shielded and a chemical shift around 25 ppm is typically observed.

For the proton chemical shifts an analogous pattern is generally assumed for the assignment of the methylene protons; it was found however, that this assumption is incorrect (see NMR‡). HMQC experiments indicate a correlation between the downfield α-carbon and the upfield methylene protons. The upfield β-carbon in turn is found to be correlated with the downfield methylene signal. This was observed for all tryptamine free base derivatives. Further confirmation was obtained by the performance of long-range ^{1}H–^{13}C COSY experiments (HMBC). Tryptamine derivative **7a** (5-MeO-DIPT) is used as a representative example as indicated in Table 10: The upfield methylene protons (CH_2-α) are correlated to the β-carbon (two-bond coupling), the isopropyl group-derived N–CH carbon (three-bond coupling) and quaternary carbon 3 on the indole ring (weak three-bond coupling). The downfield methylene protons exhibited a three-bond coupling with indole carbons 2 and 3a and a two-bond

Table 8 ^{13}C-NMR chemical shifts (in d_6-DMSO at 100 MHz, unless otherwise stated) δ of the indolic carbons of the synthesised tryptamines **1a–25a** in ppm

Compound[a]	C-2	C-3	C-3a	C-4	C-5	C-6	C-7	C-7a
5-Methoxy								
1a[b]	123.3	112.8	127.8	100.3	153.2	111.2	112.3	131.6
3a[b]	123.3	112.7	127.8	100.4	153.2	111.2	112.3	131.5
5a[b]	123.4	112.8	127.8	100.2	153.2	111.2	112.3	131.8
7a	123.3	113.0	127.8	100.4	153.1	111.1	112.3	131.5
9a	123.5	112.7	127.9	100.5	153.2	111.2	112.3	131.7
11a[b]	123.4	112.8	127.9	100.4	153.2	111.2	112.3	131.7
13a	123.5	113.1	127.9	100.4	153.2	111.6	112.3	131.7
15a[b]	123.4	112.9	127.9	100.4	153.2	111.2	112.3	131.7
17a	123.5	112.8	127.9	100.5	153.2	111.3	112.3	131.8
18a[b]	123.4	112.8	127.9	100.5	153.2	111.2	112.2	131.7
20a[b]	123.3	112.8	127.8	100.4	153.2	111.2	112.3	131.6
22a	123.5	113.0	127.9	100.4	153.2	111.2	112.3	131.7
24a[b]	123.4	112.8	127.9	100.5	153.2	111.2	112.3	131.7
Unsubstituted								
2a	122.7	113.1	127.6	118.4	118.4	121.1	111.7	136.6
4a[b]	122.7	113.2	127.6	118.4[c]	118.5[c]	121.6	111.7	139.5
6a	122.7	113.0	127.6	118.4[c]	118.5[c]	121.1	111.7	139.5
8a	122.7	113.4	127.7	118.5	118.5	121.0	111.7	136.5
10a	122.8	112.9	127.6	118.5[c]	118.6[c]	121.1	111.7	136.5
12a	122.8	113.1	127.6	118.4	118.4	121.1	111.7	136.6
14a	122.8	113.3	127.7	118.4[c]	118.5[c]	121.1	111.7	136.5
16a	122.6	113.0	127.5	118.4[c]	118.5[c]	121.2	111.6	136.4
19a[b]	122.7	113.1	127.6	118.4[c]	118.5[c]	121.6	111.7	136.6
21a[b]	122.9	112.6	127.5	118.5	118.5	121.2	111.7	136.5
23a	122.8	113.2	127.6	118.4[c]	118.6[c]	121.1	111.7	136.5
25a	122.7	113.0	127.6	118.4[c]	118.6[c]	121.1	111.7	136.6

[a] The top group of compounds are for the 5-methoxy-*N*,*N*-disubstituted tryptamines, whereas the bottom group of compounds are for the unsubstituted *N*,*N*-disubstituted tryptamines (5-H). [b] 75 MHz. [c] C-5/C-4 may be interchanged.

Table 9 ^{1}H-NMR chemical shifts (in d_6-DMSO at 300 MHz, unless otherwise stated) δ of the indolic protons of the synthesised tryptamines **1a–25a** in ppm

Compound[a]	NH-1, mu[b]	H-2, mu, J[c]	H-4, mu, J	H-5, mu, J	H-6, mu, J	H-7, mu, J
5-Methoxy						
1a	10.60, br s	7.09, d, 2.3	6.94, d, 2.3	—	6.71, dd, 8.7, 2.3	7.22, d, 8.7
3a	10.61, br s	7.10, d, 2.3	6.96, d, 2.3	—	6.71, dd, 8.9, 2.4	7.22, d, 8.7
5a	10.59, br s	7.07, d, 1.8	6.91, d, 2.3	—	6.71, dd, 8.7, 2.6	7.22, d, 8.7
7a	10.62, br s	7.09, s	6.92, d, 2.3	—	6.71, dd, 8.7, 2.3	7.22, d, 8.7
9a[d]	10.63, br s	7.10, d, 2.5	6.97, d, 2.5	—	6.71, dd, 8.5, 2.5	7.22, d, 9.0
11a	10.60, br s	7.08, d, 1.9	6.93, d, 2.3	—	6.71, dd, 8.7, 2.3	7.22, d, 8.7
13a	10.60, br s	7.10, d, 2.0	6.97, d, 2.3	—	6.71, dd, 8.7, 2.5	7.22, d, 8.7
15a	10.63, br s	7.09, d, 1.9	6.95, d, 2.6	—	6.71, dd, 8.9, 2.4	7.22, d, 8.7
17a[d]	10.63, br s	7.09, d, 2.3	6.98, d, 2.3	—	6.71, dd, 8.5, 2.4	7.22, d, 8.7
18a	10.60, br s	7.09, br s	6.97, d, 2.3	—	6.71, dd, 8.7, 2.3	7.23, d, 9.0
20a	10.61, br s	7.10, d, 2.3	6.95, d, 2.3	—	6.71, dd, 8.9, 2.5	7.22, d, 8.7
22a[d]	10.61, br s	7.10, d, 2.5	6.97, d, 2.0	—	6.71, dd, 8.8, 2.3	7.23, d, 9.0
24a	10.61, br s	7.10, d, 2.3	6.97, d, 2.3	—	6.71, dd, 8.7, 2.3	7.23, d, 8.7
Unsubstituted						
2a	10.74, br s	7.12, s	7.47, d, 7.9	6.96, t, 7.7	7.05, t, 7.5	7.32, d, 7.9
4a	10.76, br s	7.13, d, 2.5	7.47, d, 7.9	6.96 , t, 7.3	7.05, t, 7.3	7.33, d, 7.9
6a[d]	10.76, br s	7.12, d, 2.0	7.47, d, 8.0	6.97, td, 7.5, 1.0	7.05, td, 7.5, 1.0	7.33, d, 8.0
8a	10.77, br s	7.14, d, 1.9	7.48, d, 7.9	6.98, t, 7.3	7.06, t, 7.5	7.34, d, 7.9
10a	10.77, br s	7.14, d, 2.0	7.51, d, 7.9	6.97, td, 7.5, 1.0	7.06, td, 7.5, 1.0	7.33, d, 8.3
12a[d]	10.76, br s	7.14, d, 2.0	7.48, d, 8.0	6.97, td, 7.5, 1.0	7.05, td, 7.5, 1.0	7.33, d, 8.0
14a[d]	10.77, br s	7.14, d, 2.5	7.48, d, 8.0	6.97, td, 7.5, 1.0	7.05, td, 7.5, 1.5	7.33, d, 8.0
16a	10.77, br s	7.13, d, 1.9	7.49, d, 7.2	6.97, td, 7.3, 1.1	7.06, td, 7.5, 1.1	7.34, d, 8.3
19a	10.78, br s	7.14, d, 1.9	7.51, d, 7.5	6.97, t, 7.5	7.07, t, 7.5	7.34, d, 8.7
21a	10.80, br s	7.15, d, 1.9	7.51, d, 7.5	6.97, td, 7.3, 1.1	7.06, td, 7.5, 1.1	7.34, d, 7.9
23a[d]	10.77, br s	7.14, d, 2.3	7.49, d, 7.5	6.97, t, 7.3	7.06, t, 7.3	7.33, d, 8.0
25a[d]	10.76, br s	7.14, d, 2.3	7.50, d, 7.8	6.97, td, 7.0, 1.0	7.06, td, 6.9, 1.3	7.34, d, 8.0

[a] The top group of compounds are for the 5-methoxy-*N*,*N*-disubstituted tryptamines, whereas the bottom group of compounds are for the unsubstituted *N*,*N*-disubstituted tryptamines (5-H). [b] Multiplicity. [c] Coupling constant in Hz. [d] 400 MHz.

correlation with the α-carbon and indole carbon 3. It is also apparent that according to the 2D-correlations the proton chemical shifts of the methylene protons do not show solvent dependency. This is reflected by the fact that in case of a tryptamine free base derivative the methylene CH_2-β protons resonate always further downfield when compared with their CH_2-α counterparts in the ^{1}H-NMR spectrum. As exemplified by the hydrochloride-, fumarate- and monooxalate salt of **7a** however, the downfield methylene protons are correlated to the α-carbons which suggests an interchange of the methylene proton assignments between free base and salt (Table 10).

Conclusion

This detailed study of intermediates and products in the Speeter and Anthony synthetic route to symmetrically and asymmetrically substituted *N*,*N*-dialkyltryptamines has revealed the possibility of determining their presence in samples found during criminal investigations, and in preparations made for clinical investigations. The synthesis, NMR and MS characterisation of these compounds provides the forensic analyst and clinical biochemist with a detailed and self-consistent set of data and mechanisms for the spectral identification of the more likely psychoactive tryptamines that may be met. The NMR work has shown a solvent dependency that has to be taken into consideration for the unambiguous assignment of ^{1}H- and ^{13}C-NMR chemical shifts. The ^{1}H-NMR study demonstrated that one can evaluate the rotamer populations of the unsymmetrical glyoxalylamides.

This study coupled with the earlier work[23] provides the means to identify both the synthetic route and potential

Table 10 Influence of the solvents on the chemical shift of the methylene protons of 5-methoxy-*N*,*N*-diisopropyltryptamine (**7a**)[na]

	CH_2-α				CH_2-β		
Compd. **7a**	Solvent	δ ^{13}C	δ ^{1}H, mu[nc]	HMBC to C# CH_2-α	δ ^{13}C	δ ^{1}H, mu[nc]	HMBC to C# CH_2-β
Free base	d_6-DMSO	46.3	2.64–2.59, m	CH_2-β, N–CH, 3	27.9	2.71–2.67, m	CH_2-α, 3, 2, 3a
Free base	$CDCl_3$	47.0	2.76–2.69, m	CH_2-β, N–CH, 3	28.6	2.88–2.81, m	CH_2-α, 3, 2, 3a
Free base	CD_3OD	47.5	2.75–2.68, m	CH_2-β, N–CH, 3[nd]	28.0	2.85–2.79, m	CH_2-α, 3, 2, 3a
Hydrochloride	CD_3OD	48.2	3.37–3.32, m	CH_2-β, N–CH, 3	23.8	3.21–3.16, m	CH_2-α, 3, 2, 3a
Hydrochloride	d_6-DMSO	47.0	3.26–3.22, m	CH_2-β, N–CH, 3	22.7	3.12–3.08, m	CH_2-α, 3, 2, 3a
Fumarate	d_6-DMSO	47.2	3.22–3.15, m	CH_2-β, N–CH, 3[nd]	23.4	3.07–3.00, m	CH_2-α, 3, 2, 3a
Monooxalate	d_6-DMSO	47.3	3.24–3.19, m	CH_2-β, N–CH, 3[nd]	23.2	3.07–3.02, m	CH_2-α, 3, 2, 3a

[a] Only in the case of a salt the CH_2-α protons are found to be more deshielded than their vicinal CH_2-β protons as confirmed by HMQC and HMBC experiments (see text) [b] 300 MHz, in d_6-DMSO relative to residual solvent at 2.51 ppm, others relative to TMS. [c] Multiplicity. [d] Weak coupling.

impurities even in quite complex and impure products. The mass spectral analysis demonstrated the capability of positive-ion electrospray tandem mass spectrometry to generate diagnostically useful fragment ions that are partially identical with fragment ions observed in electron ionisation spectra. The convenient application of flow injection analysis in combination with in-source CID and ESI-TQ-MS-MS provides sufficient mass spectral information to identify and distinguish isomeric tryptamine derivatives without the necessity of previous separations. The use of tandem mass spectral methodologies may offer several advantages in terms of specificity and sensitivity. Indeed, it is known that several psychoactive tryptamines such as 5-HO-DMT, DMT and 5-MeO-DMT are found in mammalian systems. The use of these new methodologies is expected to contribute both to any forensic investigation and to a more detailed understanding of the significance of the presence of these compounds in man.[56–58]

Acknowledgements

SDB and PMcG are supported by UMIST with a Departmental Scholarship. Much of the GC, LC and MS equipment was purchased under the Scientific Research Infrastructure Fund Initiative. We thank Eric Warburton, UMIST, for performing exact mass measurements and Mark Hillmer, Varian Ltd., for assistance with the instrumentation. The work was carried out under a Home Office licence.

Simon D. Brandt,[a] Sally Freeman,[b] Ian A. Fleet,[c] Peter McGagh[a] and John F. Alder*[a]

[a]Department of Instrumentation and Analytical Science, UMIST, Manchester, UK M60 1QD. E-mail: fred.alder@umist.ac.uk; Fax: +44 161 200 4881; Tel: +44 161 200 4885

[b]School of Pharmacy and Pharmaceutical Sciences, University of Manchester, Oxford Road, Manchester, UK M13 9PL. E-mail: sally.freeman@man.ac.uk

[c]Department of Chemistry, UMIST, Manchester, UK M60 1QD

References

1 R. E. Schultes and A. Hofmann, *The Botany and Chemistry of Hallucinogens*, Charles C. Thomas, Springfield, Illinois, USA, 1980.
2 R. E. Schultes and A. Hofmann, *Plants of the Gods: Their Sacred, Healing and Hallucinogenic Powers*, Healing Arts Press, Rochester, VT, 1992.
3 R. J. Strassman and C. R. Qualls, *Arch. Gen. Psychiatry*, 1994, **51**, 85.
4 R. J. Strassman, C. R. Qualls, E. H. Uhlenhuth and R. Kellner, *Arch. Gen. Psychiatry*, 1994, **51**, 98.
5 R. J. Strassman, *Behav. Brain Res.*, 1996, **73**, 121.
6 D. J. McKenna, *Pharmacol. Ther.*, 2004, **102**, 111.
7 E. Gouzoulis-Mayfrank, K. Heekeren, B. Thelen, H. Lindenblatt, K. A. Kovar, H. Sass and M. A. Geyer, *Behav. Pharmacol.*, 1998, **9**, 561.
8 F. X. Vollenweider and M. A. Geyer, *Brain Res. Bull.*, 2001, **56**, 495.
9 F. Hasler, U. Grimberg, M. A. Benz, T. Huber and F. X. Vollenweider, *Psychopharmacology*, 2004, **172**, 145.
10 D. E. Nichols, *Pharmacol. Ther.*, 2004, **101**, 131.
11 A. T. Shulgin and A. Shulgin, *TIHKAL: The Continuation*, Transform Press, Berkeley, 1997.
12 J. Ott, *J. Psychoact. Drugs*, 2001, **33**, 273.
13 J. Ott, *J. Psychoact. Drugs*, 2001, **33**, 403.
14 A. T. Shulgin, in *Hallucinogens. A Forensic Drug Handbook*, ed. R. R. Laing, Elsevier Science Ltd., London, 2003, p. 67.
15 J. F. Van Bocxlaer, K. M. Clauwaert, W. E. Lambert, D. L. Deforce, E. G. Van den Eeckhout and A. P. De Leenheer, *Mass Spectrom. Rev.*, 2000, **19**, 165.
16 M. J. Bogusz, *J. Chromatogr. B: Biomed. Sci. Appl.*, 2000, **748**, 3.
17 P. Marquet, *Ther. Drug Monit.*, 2002, **24**, 255.
18 K. Pihlainen, E. Sippola and R. Kostiainen, *J. Chromatogr. A*, 2003, **994**, 93.
19 M. J. Bogusz, R. D. Maier, A. T. Schafer and M. Erkens, *Int. J. Legal Med.*, 1998, **111**, 147.
20 T. Kamata, M. Nishikawa, M. Katagi and H. Tsuchihashi, *J. Chromatogr. B*, 2003, **796**, 421.
21 M. E. Speeter and W. C. Anthony, *J. Am. Chem. Soc.*, 1954, **76**, 6208.
22 S. Freeman and J. F. Alder, *Eur. J. Med. Chem.*, 2002, **37**, 527.
23 S. D. Brandt, S. Freeman, I. A. Fleet, P. McGagh and J. F. Alder, *Analyst*, 2004, **129**, 1047.
24 J. C. Powers, *J. Org. Chem.*, 1968, **33**, 2044.
25 S. W. Bellman, J. W. Turczan and T. C. Kram, *J. Forensic Sci.*, 1970, **15**, 261.
26 M. W. Couch and C. M. Williams, *Anal. Biochem.*, 1972, **50**, 612.
27 S. E. Hattox and R. C. Murphy, *Biomed. Mass Spectrom.*, 1975, **2**, 272.
28 G. J. Shaw, G. J. Wright and G. W. Milne, *Biomed. Mass. Spectrom.*, 1977, **4**, 348.
29 B. Holmstedt and J. E. Lindgren, in *Ethnopharmacologic Search for Psychoactive Drugs*, ed. D. H. Efron, B. Holmstedt and N. S. Kline, (Reprint), Raven Press, New York, 1979, p. 339.
30 J. H. Beynon R. A. Saunders and A. E. Williams, *The Mass Spectra of Organic Molecules*, Elsevier, Amsterdam, Netherlands, 1968.
31 G. Diamantini, G. Tarzia, G. Spadoni, M. D'Alpaos and P. Traldi, *Rapid Commun. Mass Spectrom.*, 1998, **12**, 1538.
32 T. R. Bosin, T. L. Harrison and S. D. Jr., *Res. Commun. Chem. Pathol. Pharmacol.*, 1974, **7**, 519.
33 D. G. I. Kingston, J. T. Bursey and M. M. Bursey, *Chem. Rev.*, 1974, **74**, 215.
34 J. Gynther, *Acta Chem. Scand. B*, 1988, **B42**, 433.
35 R. D. Bowen, *Mass Spectrom. Rev.*, 1991, **10**, 225.
36 H. J. Veith and J. H. Gross, *Org. Mass Spectrom.*, 1991, **26**, 1097.
37 R. D. Bowen, *J. Chem. Soc., Perkin Trans. 2*, 1993, **12**, 2363.
38 R. D. Bowen, *J. Chem. Soc., Perkin Trans. 2*, 1993, **3**, 285.
39 T. I. Solling and S. Hammerum, *J. Chem. Soc., Perkin Trans. 2*, 2001, 2324.
40 R. D. Bowen, *J. Chem. Soc., Perkin Trans. 2*, 1982, **4**, 409.
41 S. J. Mandeville, R. D. Bowen, M. A. Trikoupis and J. K. Terlouw, *Int. J. Mass Spectrom.*, 2000, **199**, 189.
42 S. McClean, R. C. Robinson, C. Shaw and W. F. Smyth, *Rapid Commun. Mass Spectrom.*, 2002, **16**, 346.
43 H. Budzikiewicz, C. Djerassi and D. H. Williams, *Mass Spectrometry of Organic Compounds*, Holden-Day, San Francisco, 1967.
44 P. Rösner and T. Junge, *J. Mass Spectrom.*, 1996, **31**, 1047.
45 L. M. Jackman, in *Dynamic Nucluear Magnetic Resonance Spectroscopy*, ed. L. M. Jackman and F. A. Cotton, Academic Press, New York, 1975, p. 203.
46 W. E. Stewart and T. H. Siddall, III, *Chem. Rev.*, 1970, **70**, 517.
47 D. B. Repke, W. J. Ferguson and D. K. Bates, *J. Heterocycl. Chem.*, 1977, **14**, 71.
48 D. B. Repke, W. J. Ferguson and D. K. Bates, *J. Heterocycl. Chem.*, 1981, **18**, 175.
49 D. B. Grotjahn, *J. Heterocycl. Chem.*, 1983, **20**, 1031.
50 M. Spaeth, P. Plischka, F. M. Bohnen, R. Herbst-Irmer and H. Laatsch, *J. Prakt. Chem.*, 1997, **339**, 243.
51 M. S. Morales-Ríos, R. E. del Rio and P. Joseph-Nathan, *Magn. Reson. Chem.*, 1989, **27**, 1039.
52 A. A. Tymiak, K. L. Rinehart and G. J. Bakus, *Tetrahedron*, 1985, **41**, 1039.

53 P. Joseph-Nathan, R. E. del Rio and M. S. Morales-Ríos, *Heterocycles*, 1988, **27**, 377.
54 M. S. Morales-Rios and P. Joseph-Nathan, *J. Heterocycl. Chem.*, 1986, **23**, 1617.
55 M. S. Morales-Ríos, J. Espineira and P. Joseph-Nathan, *Magn. Reson. Chem.*, 1987, **25**, 377.
56 S. A. Barker, J. A. Monti and S. T. Christian, *Int. Rev. Neurobiol.*, 1981, **22**, 83.
57 S. A. Barker, M. A. Littlefield-Chabaud and C. David, *J. Chromatogr. B: Biomed. Sci. Appl.*, 2001, **751**, 37.
58 T. Forsström, J. Tuominen and J. Karkkainen, *Scand. J. Clin. Lab. Invest.*, 2001, **61**, 547.